Numerical and experimental procedure for designing sub-sea installation operations

André L. C. Fujarra[1], Eduardo A. Tannuri[2], Felipe R. Pereira[3], Rafael M. L. Madureira[4], Isaias Q. Masetti[5] and Haroldo Igreja[6]

1 Department of Naval Arch. & Ocean Eng., Numerical Offshore Tank (TPN-USP), University of São Paulo, Brazil, afujarra@usp.br

2 Department of Mechatronics Eng., Numerical Offshore Tank (TPN-USP), University of São Paulo, Brazil, eduat@usp.br

3 Department of Naval Arch. & Ocean Eng., Numerical Offshore Tank (TPN-USP), University of São Paulo, Brazil, rateiro@tpn.usp.br

4 Petrobras Transportes SA, Petrobras, Brazil, rafael.madureira@petrobras.com.br

5 Petrobras Transportes SA, Petrobras, Brazil, masetti@petrobras.com.br

6 E&P - Serv, Petrobras, Brazil, higreja@petrobras.com.br

Abstract

Sub-sea equipment installations are very complex operations, requiring pre-installation analysis to define the correct procedure and the weather "window" for a safe operation. This paper addresses the installation of a Mid Water Arch (MWA) intended to provide support to the riser. Connecting the riser to the MWA largely eliminates the dynamic forces that would otherwise cause friction and fatigue. The MWA is composed of riser guides and several buoyancy tanks and is kept in the water with tethers connected to an anchor. The installation procedure involves launching each component of the MWA (anchor, main structure and tethers), during which a tug boat with an A-frame and an assistance vessel are used to keep the buoy away from the tether and the launch cable. The waves induce oscillatory motions throughout the system and may cause large dynamic forces in the cables and tethers. Due to the complexity of the multi-body system, a comprehensive numerical and small-scale experimental analysis is conducted to calculate the proper dimensions for the launch cables and to define the limits of the environmental conditions. Numerical analysis was carried out in the Numerical Offshore Tank – TPN, a multi-processor offshore system simulator that considers the 6 degrees of freedom for each body and all environmental forces acting upon them. The lines are modeled by finite-element analysis. Furthermore, a full set of small-scale experiments were carried out at a towing tank that considered the response of the system when excited by sinusoidal motion at the top and emulated the wave excitation. Comparisons between numerical and experimental results showed good adherence between the calculated values. The validated numerical simulator was then used to analyze the complete complex installation procedure by considering an extensive set of environmental conditions.

Keywords

Subsea installation; Simulation; Offshore operation

Nomenclature

BTA	Buoyancy Tank Assembly
CG	Center of Gravity
DOF	Degree of Freedom
IPT	State of São Paulo Technological Research Institute
LVDT	Linear variable differential transformer
MWA	Mid Water Arch
TPN	Numerical Offshore Tank
RAO	Response Amplitude Operator
ROV	Remotely Operated Vehicle

Submitted to MS&OT on May 24 2010. Revised version submitted on Nov 18 2010. Accepted on Dec 10 2010. Editor: ***Celso Pesce****.*

1 Introduction

Subsea equipments such as manifolds and riser supporting systems require complex offshore operations to be launched and positioned in the correct location in the seabed. Rowe et al. (2001) presented several problems associated with subsea launching. Although the focus of that work is deepwater operations, the main concerns may be also extrapolated for all launching operations. The most relevant problems pointed by the authors are:

- Lifting equipments: problems associated with the loads to be lowered, dynamic amplification during the launch and capability of the equipments;
- Load control and positioning: problems associated with the correct final laying positioning of the subsea equipment;
- Weather conditions: problems associated with launching vessel induced motions and weather window to a safe operation.

The present paper presents a methodology to analyze complex offshore operations involving sub-sea installations and several support vessels. The execution of full-scale experiments involving all vessels and components of the actual operation may be extremely complex and expensive. Furthermore, depending on the needs of the offshore industry, the time required to prepare and execute such experiments may not make the experiments feasible.

Numerical simulation is a tool that engineers use for performing analysis prior to actual installation. Ferreira (2002) presented an extensive numerical analysis of a conventional manifold installation procedure using a linear frequency domain analysis. In that work, the importance of the coupled dynamic analysis was stressed. An alternative launching method using two vessels was presented by Santos et al, (2009). Nonlinear time domain simulation were used for predicting the loads in the cables, but no dynamic coupling between vessels and the load has been considered. In those works, no experimental validations were presented.

However, due to the enormous complexity of some operations, the engineers cannot rely only on the numerical simulation results to make important decisions. A combination of numerical and experimental analysis was presented by Fernandes et al. (2006) for the evaluation of the pendulum method for subsea launching. This launching procedure requires one vessel and no environmental condition is considered. In that case, fundamental aspects of the experimental results were recovered by simulations, but rotational motions of the manifold could not be predicted. The results obtained in the analysis were important for the definition of the real operational installation procedure (Lima et al. 2008).

This paper presents an example of a hybrid methodology to analyze a complex sub-sea equipment installation. Simplified experiments were used to validate the numerical simulations, which were then used for further complex simulations for the full-scale operation under real environmental conditions. The installation of a Mid Water Arch (MWA) is considered. The MWA is a structure that provides riser support and consists of a Buoyancy Tank Assembly (BTA), an anchor and two tethers connecting the BTA to the anchor. During the installation, supplementary cables and two tug boats are employed.

A full set of simplified and low-cost, small-scale experiments were carried out in the State of São Paulo Technological Research Institute – IPT towing tank. These results were then used to validate a numerical model developed at TPN from the University of São Paulo. Comparisons between the numerical and small-scale experimental results indicated that the numerical model was a reliable tool to predict the system's behavior during installation. Complementary numerical simulations were completed to consider extreme wave conditions and an irregular sea spectrum. The simulations indicated some operational problems that may occur during the installation, and the results were used to re-design specific steps of the procedure.

The main contribution of the paper is to present a successful case study of the hybrid methodology (simplified experiments and full time domain numerical analysis) applied to a complex subsea launching operation, under environmental conditions.

Particularly, two critical steps of the launching procedure were addressed. Case 1 was defined as the step during which the anchor is lowered through the water while the tethers remain tension free since the BTA sits on the water's surface. It is important to clarify that the anchor is supported by a lifting wire that is connected to the A-frame of the main installation vessel and the BTA is kept away from the lifting wire by the assistance vessel (see Fig. 1). Case 2 differs in that tension is added to the tethers, which pull the BTA into the water. Here again, the BTA is continuously kept away from the lifting wire by the assistance vessel, as seen in Fig. 2.

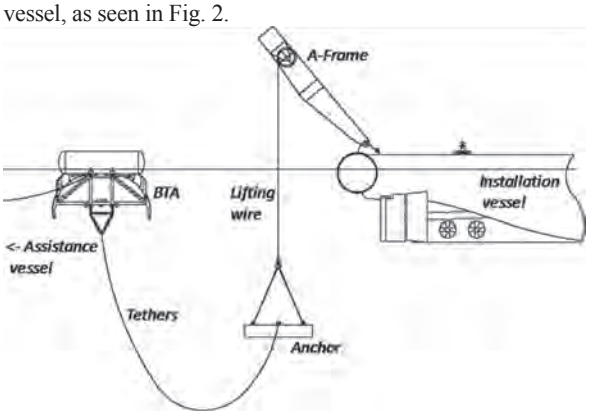

Fig. 1 The launch of the anchor - Case 1

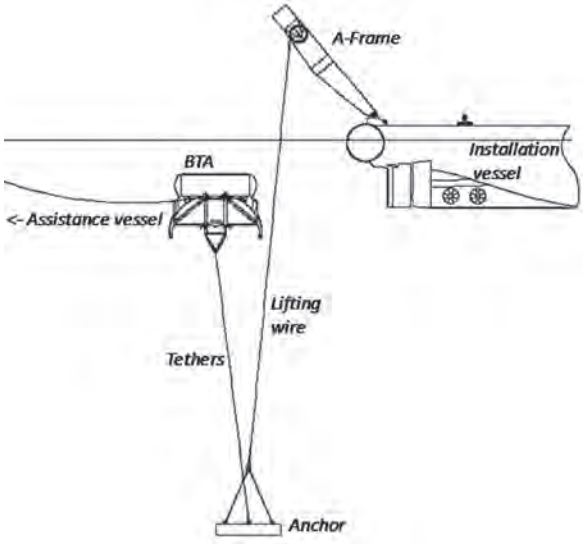

Fig. 2 The launch of the anchor connected to the BTA - Case 2

2 Modeling data

As previously mentioned, each MWA consists of a BTA, an anchor and two tethers connecting the BTA and the anchor. During the installation, supplementary cables and two tug boats are used. The technical descriptions of the equipment components and vessels involved in the operation are presented in this section. These data were used in the implementation of the numerical modeling of the operations and the experimental set-up.

The anchor is assumed to be of gravity-type and consist of a steel-reinforced concrete slab. It is equipped with two tether connection lugs and four lifting lugs. The main weight properties of the anchor are summarized in Table 1, and a principle sketch with the main dimensions is shown in Fig. 3.

Table 1 Anchor properties

Property	Value
Weight in air	1283 kN
Submerged weight	774 kN
Gross Buoyancy	509 kN

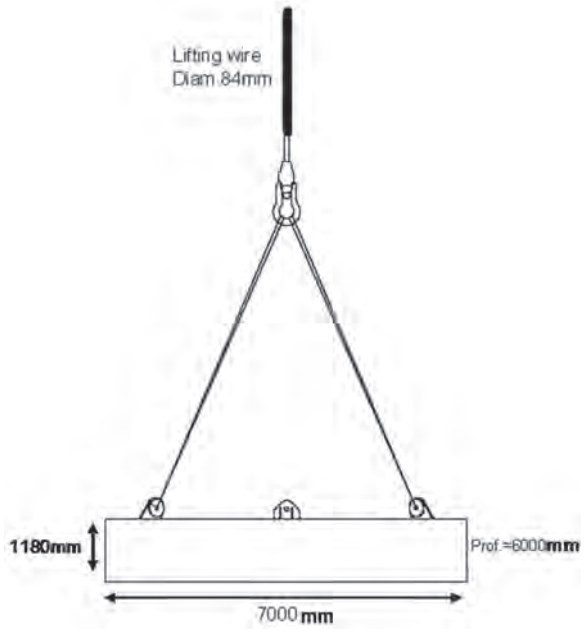

Fig. 3 Anchor and cable assembly

The BTA consists of two buoyancy tanks, a riser installation guide, a main frame steel structure, two hinged frames for tether connection and four lifting lugs for tug connection. Figure 4 presents images of the BTA during the construction, and Table 2 presents the main dimensions and weight properties of the BTA. The cables that connect the BTA to the assistance vessel during the installation of the MWA are shown in Fig. 5. Tethers of studless chain, 42m in length and 76mm in diameter, connect the anchor to the BTA. Each one weighs 48kN and presents a breaking load of 5,448kN approximately.

Table 2 BTA properties

Property	Value
Weight in air	274 kN
Net Buoyancy	529 kN
Gross buoyancy	804 kN
Length	10.2m
Width	8.4m
Height	8.6m

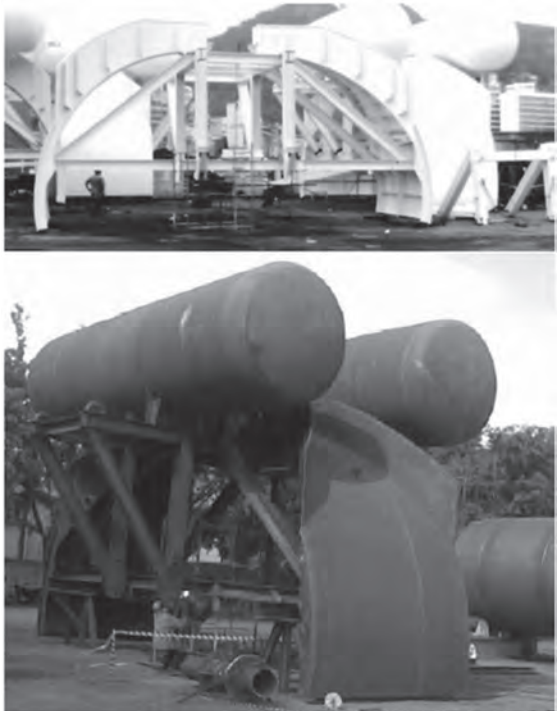

Fig. 4 Pictures of the BTA

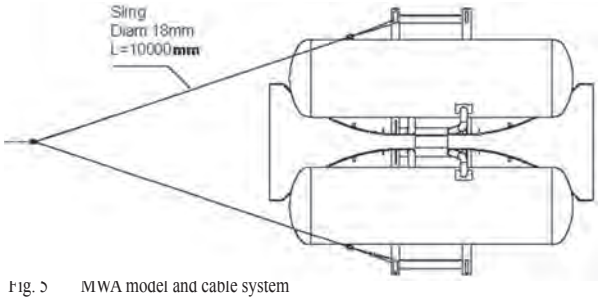

Fig. 5 MWA model and cable system

A lifting wire (launch cable) connects the anchor to the main vessel during the installation of the system. It is an 84-mm diameter steel cable with a breaking load of 4,312kN and stiffness equal to 216,300 kN/m². Two tethers connect the anchor to the BTA. They are 76-mm diameter studless chain, with 42m length and submerged weight of 44kN each.

The main installation vessel is considered to be similar to the Normand Neptun tug boat, shown in Fig. 6, and is equipped

with an A-frame for launching the anchor. According to Fig. 7, by assuming that the A-frame connection point is located 12.2m above and 47.2m from the CG, the Response Amplitude Operators (RAO's) of the vessel were obtained using the software WAMIT (WAMIT, 2000). Figure 8 presents the A-frame point heave and surge RAO for a head-sea incident wave. Large amplification of heave motion (factor 2.1) for wave periods close to 8s was verified.

Main Dimensions	
Length O.A.	80.40m
Length P.P.	69.30m
Breadth	18.00m
Depth	9.50m
Gross Tonn.	3663ton

Fig. 6 Picture and main characteristics of the Normand Neptun

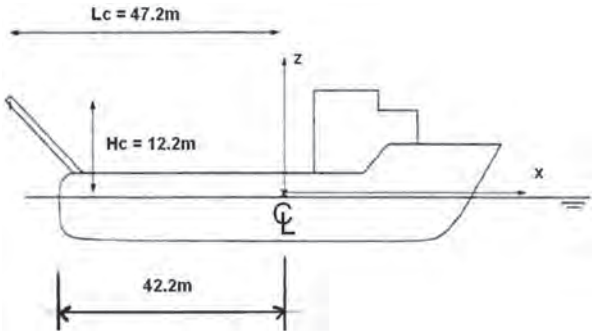

Fig. 7 Position of the A-frame in the Normand Neptun

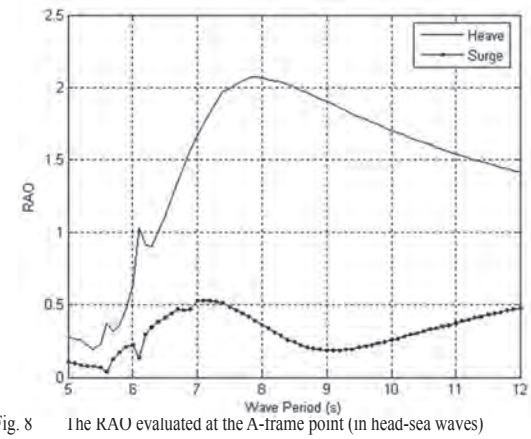

Fig. 8 The RAO evaluated at the A-frame point (in head-sea waves)

A vessel similar to the Sidney Candies tug boat has also been considered for use as the assistance installation vessel. The main characteristics of this vessel are presented in Fig. 9.

Main Dimensions	
Length O.A.	45.08m
Length P.P.	43.89m
Breadth	15.34m
Depth	6.40m

Fig. 9 Picture and main characteristics of the Sidney Candies

Head-sea waves, with 2.0m height and 9.0s peak period, were considered in the numerical and experimental analysis, for the installation location of 110m in depth.

Case 1 comprises when the anchor is being lowered through the water, and the tethers are tension free because the BTA is still on water surface. A simple static analysis revealed that the mean traction in the lifting wire would be approximately 774kN, as presented in the Fig. 10. The transition to Case 2 occurs when the tethers are under tension, while the anchor is being lowered, which pulls the BTA into the water. In both cases, the BTA is distanced from the lifting wire by the assistance vessel.

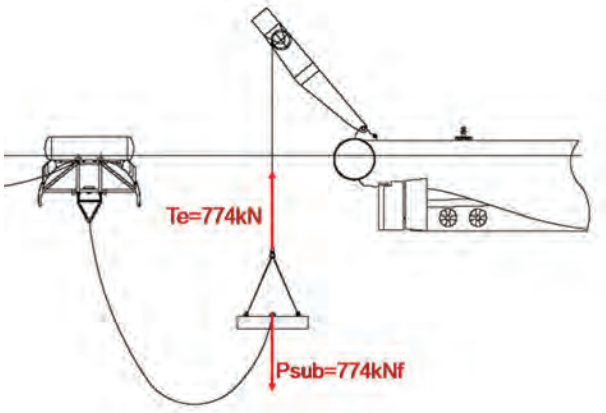

Fig. 10 Static analysis of Case 1

The static analysis was performed considering two different values for the horizontal tug force of the assistance vessel: 98kN and 196.2kN (10 and 20 ton, approximately). For the 98kN case, Fig. 11 shows the mean forces on each cable, and Fig. 12 shows the final static configuration. For the 196.2kN case, the static forces are presented in Fig. 13, and the geometrical configuration is shown in Fig. 14.

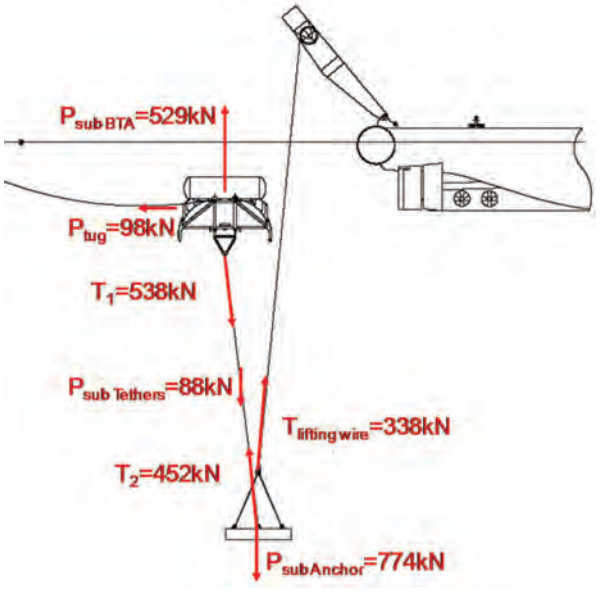

Fig. 11 Static analysis of Case 2 (98kN auxiliary tug force)

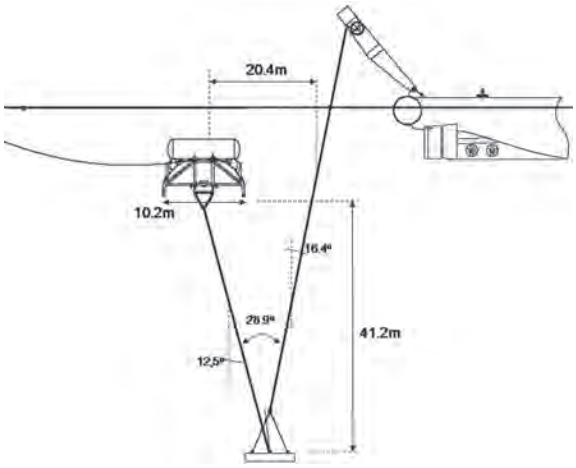

Fig. 12 Static analysis of Case 2 (98kN auxiliary tug force) – final configuration

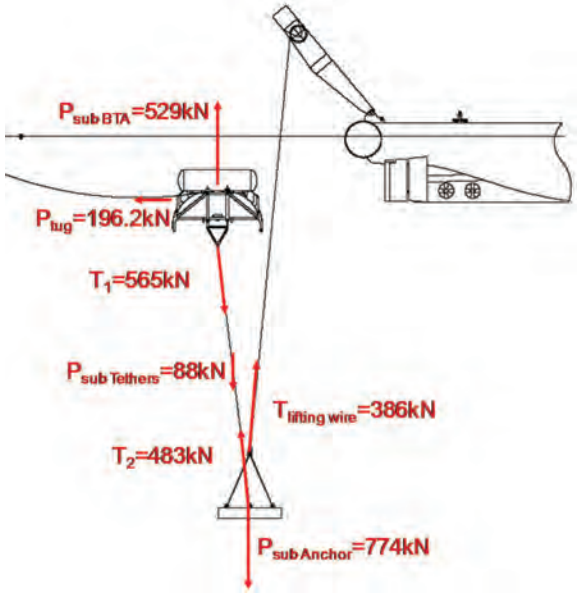

Fig. 13 Static analysis of Case 2 (196.2kN auxiliary tug force)

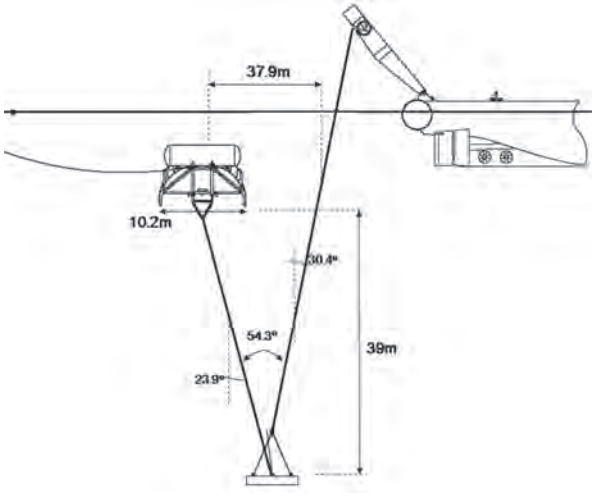

Fig. 14 Static analysis of Case 2 (196.2kN auxiliary tug force) – final configuration

The mean traction in the lifting wire increased from 338kN to 386kN when the tug force was increased from 98kN to 196.2kN, which reduced the occurrence of cable slackening during launching, as will be discussed later.

3 Experimental details

Tests were conducted at the State of São Paulo Technological Research Institute –IPT towing tank. According to the Petrobras requirements for design, four test conditions were applied:

- Case 1 - the launch of the anchor;
- Case 2 - the launch of the anchor connected to the BTA;

Considering the towing tank dimensions (6m wide and 4m deep), a scale of 1:50 was chosen for modeling the anchor, BTA and mooring system. Fig. 15 presents some photos of the anchor and BTA models. This small scale may be used to extrapolate results to full scale. The flow separation points around the anchor are well defined (since the anchor is a sharp-edge box). Therefore, the anchor drag force is weakly dependent on the Reynolds number, and is well predicted in the experiments. Furthermore, the most important dynamical effect that arises during the launching (cable slackening) is directly affected by the anchor (and not by the BTA) drag.

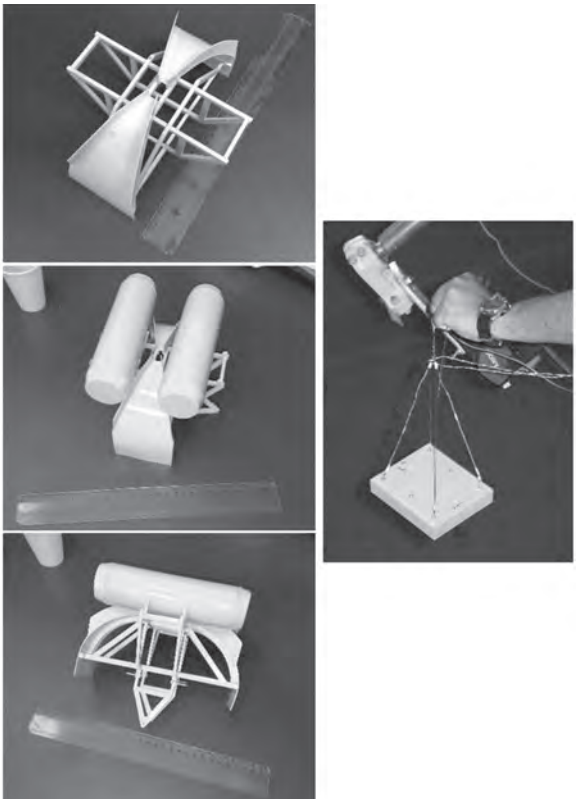

Fig. 15 Small-scale images of the anchor and BTA models (scale 1:50)

The dynamics of the tug boat during the launch were considered as equivalent vertical movements imposed by means of a servo-controlled linear actuator (see Fig. 16). Sinusoidal movements were selected and applied during the vertical movements, according to the combinations of amplitude and periods shown in the Table 3.

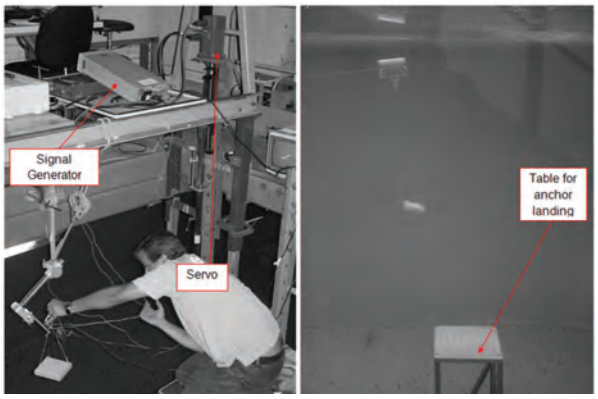

Fig. 16 Images of the servo actuator and the table for anchor landing

Table 3 Amplitude and period (Ai;Ti) combinations adopted for the sinusoidal movements imposed to the top of the launch cable. Values presented in full scale.

	T_1 = 11.78s	T_2 = 8.83s	T_3 = 5.89s
A_1 = 1.50 *m*	(A_1, T_1)	(A_1, T_2)	(A_1, T_3)
A_2 = 2.25 *m*	(A_2, T_1)	(A_2, T_2)	(A_2, T_3)
A_3 = 3.00 *m*	(A_3, T_1)	(A_3, T_2)	(A_3, T_3)

In Case 1, nine sinusoidal movements were imposed to two different lengths of the lifting wire inside the water, L = 20m and L = 60m (dimensions in full scale). In Case 2, the anchor connected to the BTA was tested for L = 60m and L = 100m. In order to emulate ground effects, a submerged table was constructed for the last depth, also shown in Fig. 16. It is important to emphasize that a grid was applied to the submerged table in order to evaluate the azimuth of the anchor landing.

Furthermore, for Case 2 conditions, two different angles between the launch line of the anchor and the tethers connecting to the BTA were considered: approximately 28° and 54°.

A load cell with fine resolution mounted on the top of the launch cable measured the time-varying traction. A LVDT was used to measure the sinusoidal movement imposed to the top end of the launch line, and two biaxial accelerometers were integrated into an internal compartment of the anchor. Tests were filmed by a set of two cameras positioned above and lateral to the experimental setup, respectively. The first camera was installed at the carriage, and the second camera filmed through the inspection window of the towing tank.

4 Experimental results

4.1 Case 1 - The launch of the anchor

First, the launch of the anchor with an imposed oscillatory movement to the top end of the launch line was considered. A photo of the anchor during the launch is shown in Fig. 17. Table 4 presents the mean, maximum and minimum forces obtained from anchor launch, as well as the respective dynamic amplification factors (defined as the relation between the maximum force and the mean force).

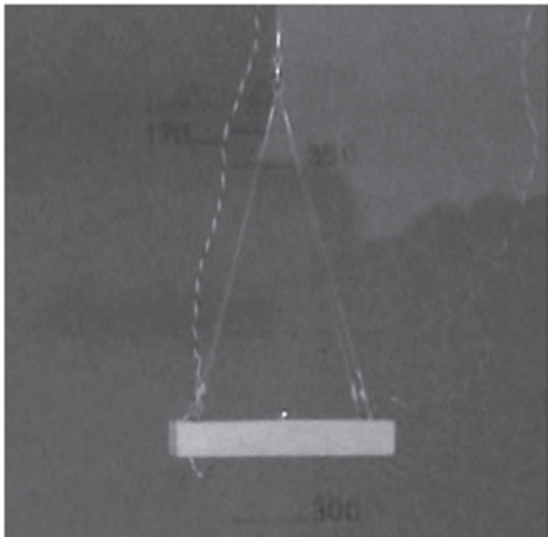

Fig. 17 Monitored anchor during the launch test – Case 1

Table 4 Results of force on the anchor (Case 1 tests).

Test	*L (m)*	*A (m)*	*T (s)*	F_{min} *(kN)*	F_{max} *(kN)*	F_{mean} *(kN)*	*Amp. Factor*
MAPH 30 06 A	60	1.5	11.78	687	824	746	1.11
MAPH 45 06 A	60	2.25	11.78	647	863	746	1.16
MAPH 60 06 A	60	3	11.78	608	883	746	1.18
MBPH 30 06 A	20	1.5	11.78	677	804	736	1.09
MBPH 45 06 A	20	2.25	11.78	638	844	746	1.13
MBPH 60 06 A	20	3	11.78	608	853	736	1.16
MAPH 30 08 A	60	1.5	8.83	628	883	755	1.17
MAPH 45 08 A	60	2.25	8.83	579	922	755	1.22
MAPH 60 08 A	60	3	8.83	510	991	755	1.31
MBPH 30 08 A	20	1.5	8.83	628	863	736	1.17
MBPH 45 08 A	20	2.25	8.83	569	903	736	1.23
MBPH 60 08 A	20	3	8.83	510	961	736	1.31
MAPH 30 12 A	60	1.5	5.89	500	1001	755	1.32
MAPH 45 12 A	60	2.25	5.89	343	1167	755	1.55
MAPH 60 12 A	60	3	5.89	186	1285	746	1.72
MBPH 30 12 A	20	1.5	5.89	481	991	746	1.33
MBPH 45 12 A	20	2.25	5.89	353	1128	746	1.51
MBPH 60 12 A	20	3	5.89	157	1265	736	1.72

In Fig. 18, the dynamic amplification factors are presented as a function of the imposed motion amplitude. As expected, when the sinusoidal amplitude increases, or the period decreases, the dynamic amplification factor increases.

According to the graphs in the Fig. 19, no combination exhibited a zero traction value in the analyzed amplitude and period ranges. The maximum force was 1285kN for 3m amplitude and 5.89s period. As a general procedure, all the time histories of force were pre-filtered in order to achieve the maximum, mean and minimum values. The pre-filtering was necessary due to high frequencies present in the signals. The signals were most

likely associated to oscillations of launch line, which was not in the same scale as the anchor and BTA models. Figure 20 compares the original and filtered time histories of force for an imposed sinusoidal movement with an amplitude and period of 1.50m and 8.83s, respectively.

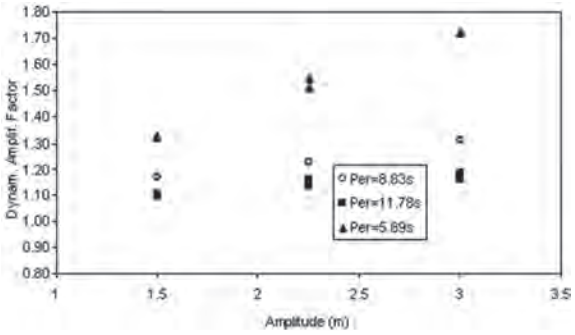

Fig. 18 Dynamic amplification factor of the force measured from above during the anchor launch

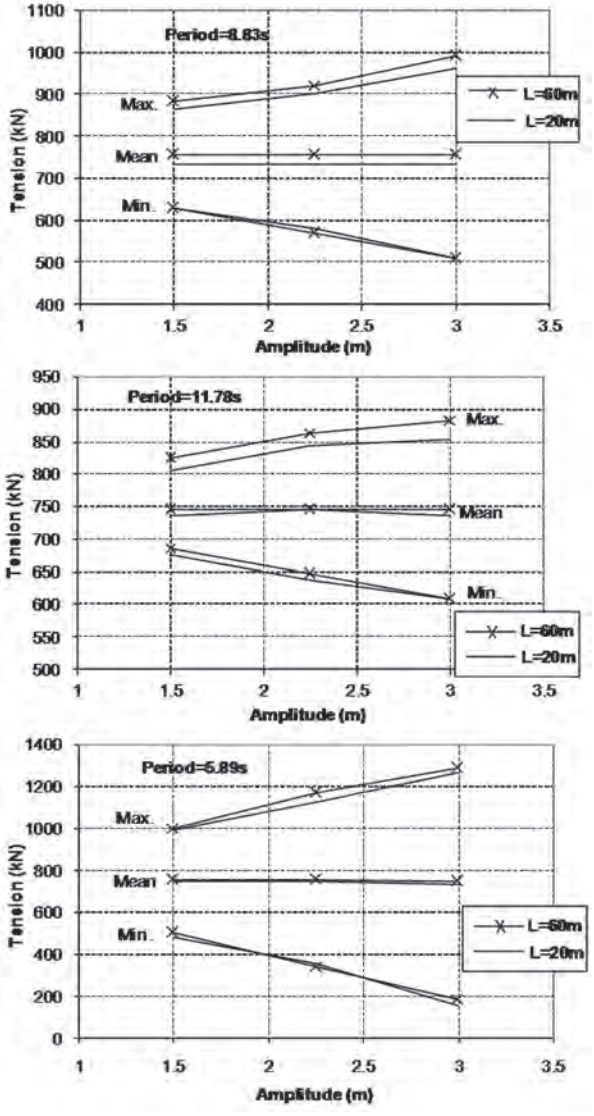

Fig. 19 Forces at the launch line during anchor installation

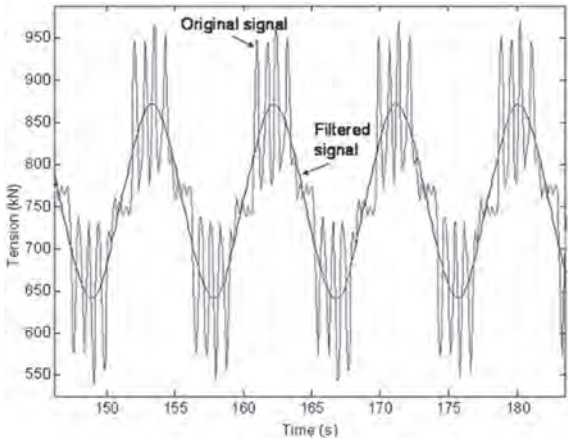

Fig. 20 Example of the force measurement for the combination MAPH3008A: the original time history and the filtered signal

Due to the heave amplification in the A-frame point (Fig. 8), a 2.00m incident wave with period 8.83s corresponds to 3.90m motion amplitude in the lifting wire. Consequently, numerical simulations (that will be detailed later) indicated a higher value of force as compared to those shown in the combinations of Table 4 combinations. In fact, the simulations of a 2.00m incident irregular wave with period 8.83s induced a maximum force of 1100kN (see Table 6). It is interesting to note that a linear extrapolation of the experimental results indicated a 1055kN of maximum force. This is consistent with that obtained in TPN simulations (see Fig. 21). Further details about the numerical simulations are found in the next section.

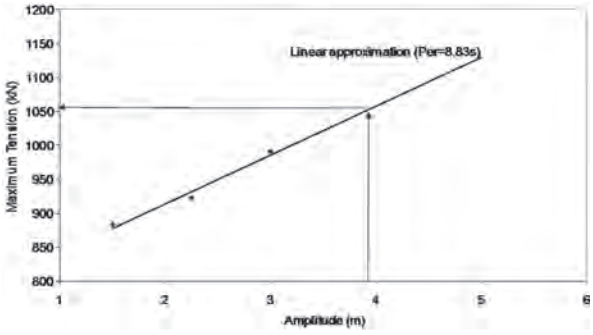

Fig. 21 Maximum forces at the launch line as function of the amplitude for the imposed sinusoidal movement. Linear extrapolation for A = 4.2m and T = 8.83s.

4.2 Case 2 - The launch of the anchor connected to the BTA

Tests were completed to examine the effects of connecting the BTA to the anchor for two different lengths of the lifting wire, 60m and 100m. The same sinusoidal movements as in Case 1 were applied to the launch line. At 60m, two static configurations were considered. The first one corresponded to an angle of approximately 28° between the launch line and the tendons connecting the BTA. These conditions were equivalent to

Faux=98kN on the line from the BTA to the assistance installation vessel. In the second configuration, Faux=196.2kN, was applied to the line connecting the BTA and the tug boat. This configuration corresponded to a 54° angle. Both geometries are presented in Fig. 22. However, only the 28° configuration was tested at 100m.

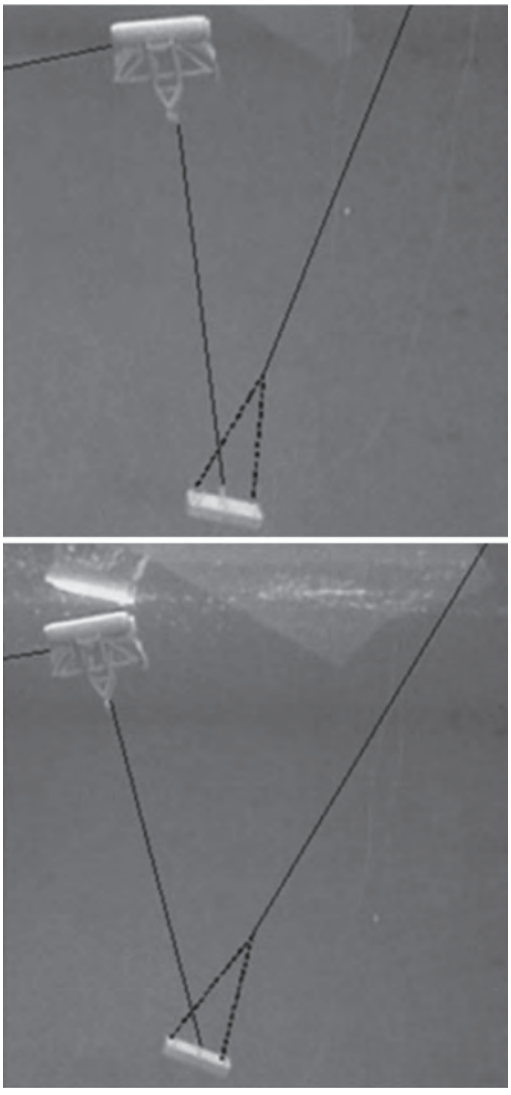

Fig. 22 Static configurations for Case 2 - the launch of the anchor connected to the BTA: angles of approximately 28° and 54°between the tendons and the l launch line.

Table 5 presents the results of all experimental configurations for Case 2. For each test, launch forces and dynamic amplification factors were obtained by the previous procedure (maximum, mean and minimum values).

Figures 23, 24 and 25 depict the forces and dynamic amplification factors as a function of the sinusoidal amplitude and the traction at the assistance installation vessel (Faux=98kN and Faux=196.2kN, respectively). The graphs consider both configurations at L=60m, as well as the three periods of movement. As expected, as the amplitude of movement increases, the associated dynamic forces and amplification factor are amplified. The higher forces were observed for 5.89s period.

Table 5 Results of force on the Case 2 tests.

Test	L(m)	A(m)	T(s)	F_{aux} (kN)	F_{min} (kN)	F_{max} (kN)	F_{mean} (kN)	Amp. Factor
BEPA 30 06 30 A	60	1.5	11.79	98	135	432	252	1.71
BEPA 45 06 30 A	60	2.25	11.79	98	83	467	252	1.85
BEPA 60 06 30 A	60	3	11.79	98	54	487	252	1.93
BEPA 30 06 60 A	60	1.5	11.79	196.2	188	411	280	1.47
BEPA 45 06 60 A	60	2.25	11.79	196.2	143	439	280	1.57
BEPA 60 06 60 A	60	3	11.79	196.2	121	457	280	1.63
BEPA 30 08 30 A	60	1.5	8.83	98	54	517	252	2.05
BEPA 45 08 30 A	60	2.25	8.83	98	25	775	253	3.06
BEPA 60 08 30 A	60	3	8.83	98	-1	1275	256	4.98
BEPA 30 08 60 A	60	1.5	8.83	196.2	120	467	281	1.66
BEPA 45 08 60 A	60	2.25	8.83	196.2	73	600	280	2.15
BEPA 60 08 60 A	60	3	8.83	196.2	34	930	280	3.33
BEPA 30 12 30 A	60	1.5	5.89	98	11	1501	255	5.88
BEPA 45 12 30 A	60	2.25	5.89	98	-16	2345	265	8.85
BEPA 60 12 30 A	60	3	5.89	98	-23	2865	272	10.54
BEPA 30 12 60 A	60	1.5	5.89	196.2	54	1236	284	4.34
BEPA 45 12 60 A	60	2.25	5.89	196.2	13	1972	293	6.72
BEPA 60 12 60 A	60	3	5.89	196.2	0	2551	302	8.44
BEPD 30 06 30 A	100	1.5	11.79	98	118	435	232	1.87
BEPD 45 06 30 A	100	2.25	11.79	98	69	461	232	1.99
BEPD 60 06 30 A	100	3	11.79	98	39	609	232	2.63
BEPD 30 08 30 A	100	1.5	8.83	98	58	677	232	2.92
BEPD 45 08 30 A	100	2.25	8.83	98	21	1015	232	4.38
BEPD 60 08 30 A	100	3	8.83	98	2	1512	235	6.43
BEPD 30 12 30 A	100	1.5	5.89	98	14	1549	235	6.59
BEPD 45 12 30 A	100	2.25	5.89	98	-4	2234	242	9.23
BEPD 60 12 30 A	100	3	5.89	98	-51	2738	239	11.45

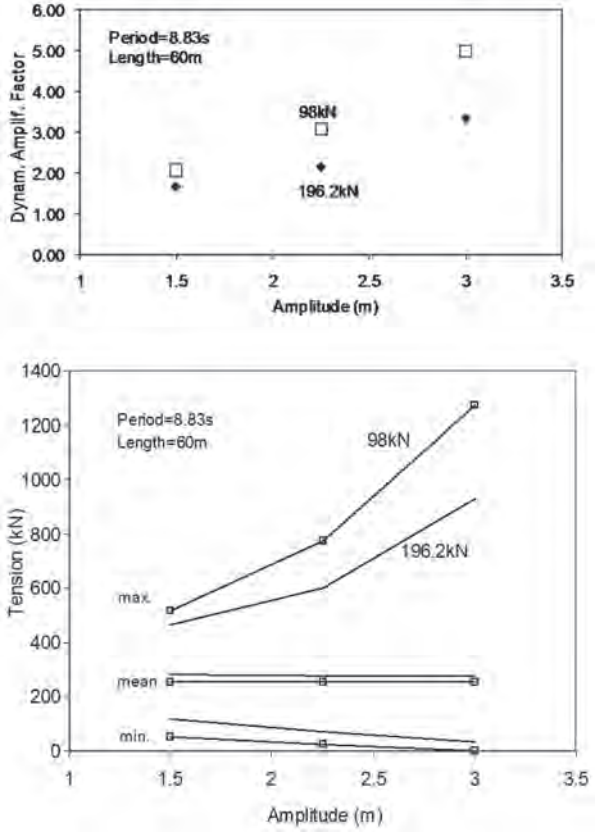

Fig. 23 (a) Dynamic amplification factor and
(b) Values of the force at the anchor launch line with length L = 60m for sinusoidal movements with period T = 8.83s.

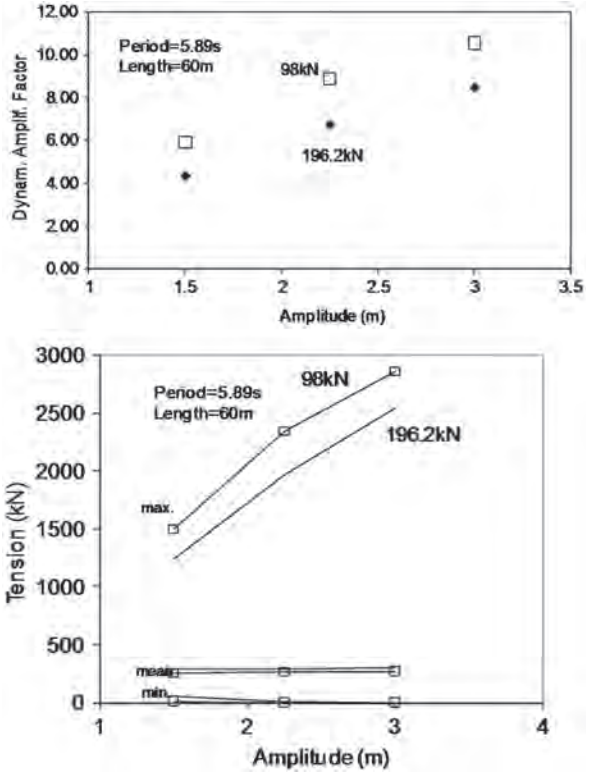

Fig. 24 (a) Dynamic amplification factor and (b) Values of force at the anchor launch line with length L = 60m for sinusoidal movements with a period of T = 5.89s.

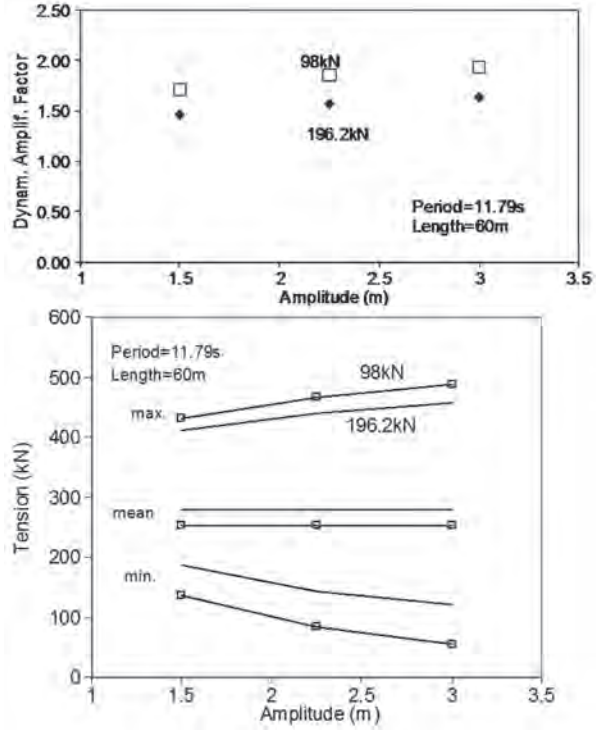

Fig. 25 - (a) Dynamic amplification factor and (b) Values of force at the launch line of anchor with length L = 60m for the sinusoidal movements with a period of T = 11.79s.

Additionally, it was verified that by increasing the assistance installation vessel force, a reduction of the dynamic amplification factor could be observed. Such a behavior can be better distinguished by comparing the graphs in Fig. 26, where force time histories at the launch line are presented for both cases of auxiliary tug force (98kN and 196.2kN, respectively) at two different periods of imposed movement.

Figures 27, 28 and 29 present the cases of an auxiliary tug force of 98kN, at two values of lifting wire length (L), 60m and 100m. As the depth increased there was a reasonable amplification of the traction at the launch line of the anchor. The same conclusion could be obtained though observation of Fig. 30, which compares the tests from different periods.

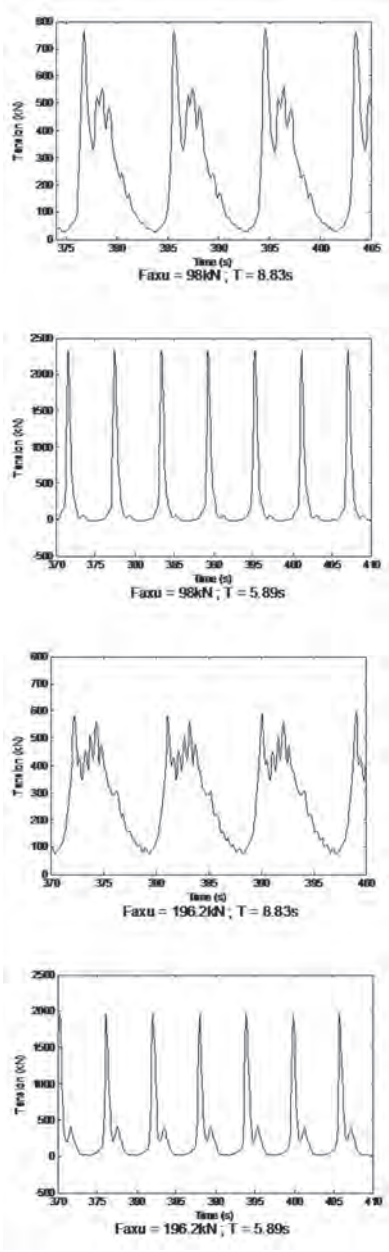

Fig. 26 Time histories of force at the launch line for a 2.25-m amplitude and lifting line length of 60m.

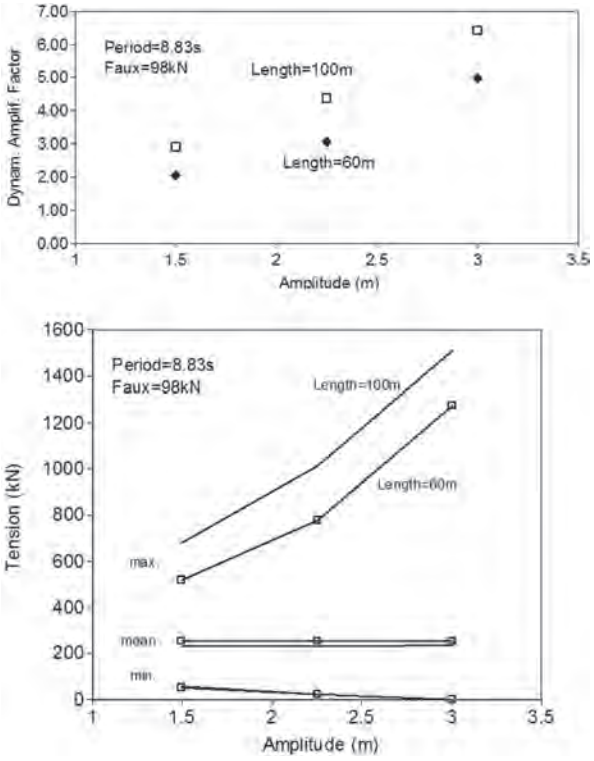

Fig. 27 (a) Dynamic amplification factor and (b) Values of force at the anchor launch line, for period T = 8.83s, Faux = 98kN and two values of line length (60m and 100m).

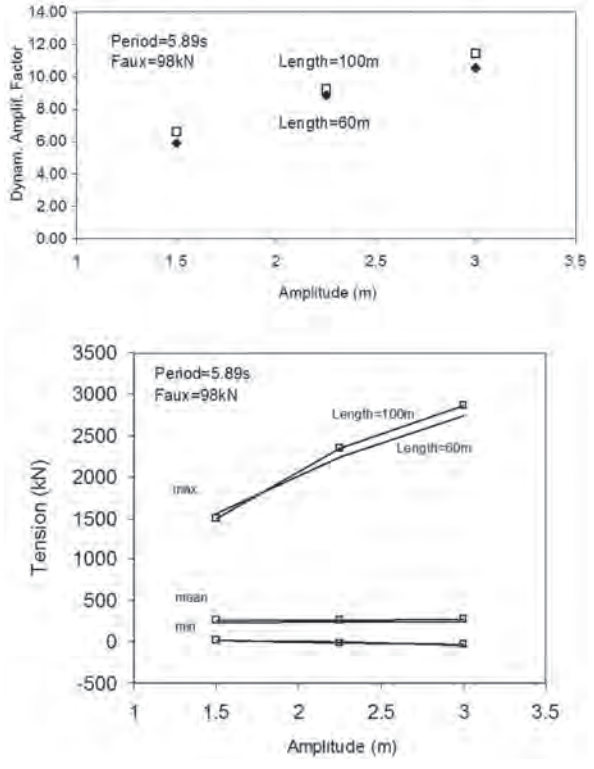

Fig. 28 (a) Dynamic amplification factor and (b) Values of force at the launch line of anchor for period T = 5.89s, Faux = 98kN and two values of line length (60m and 100m).

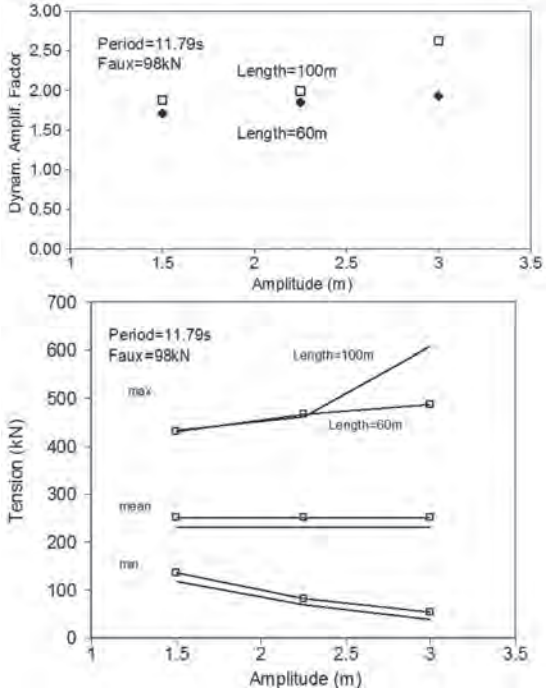

Fig. 29 (a) Dynamic amplification factor and (b) Values of force at the anchor launch line for period T = 11.79s, Faux = 98kN and two values of line length (60m and 100m).

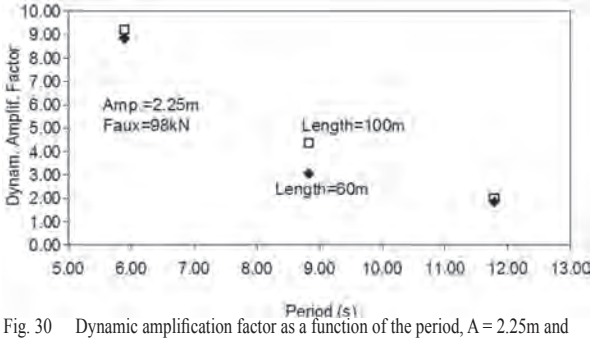

Fig. 30 Dynamic amplification factor as a function of the period, A = 2.25m and Faux = 98kN.

5 Numerical analysis and validation

Numerical models of the MWA launching procedure were programmed in the Numerical Offshore Tank – TPN. The TPN is a multi-processor offshore system simulator that considers the 6DOF for each body and all environmental forces acting in them, as well as complex finite element models for the cables and mooring lines (Nishimoto et al, 2003). A full description of the models included in TPN is given in the Appendix.

Simulations with the same conditions as the experimental cases were carried out, in order to validate the numerical models with the pre-existing small-scale experiments. After comparable results were verified between both methods, simulations involving irregular waves were performed. This allowed for evaluation of the behavior of the actual system during offshore operation.

5.1 Case 1 - The launch of the anchor

The launch of the anchor was simulated with several differing lengths of lifting wire. An example of the 3-D view of the numerical model is show in Fig. 31.

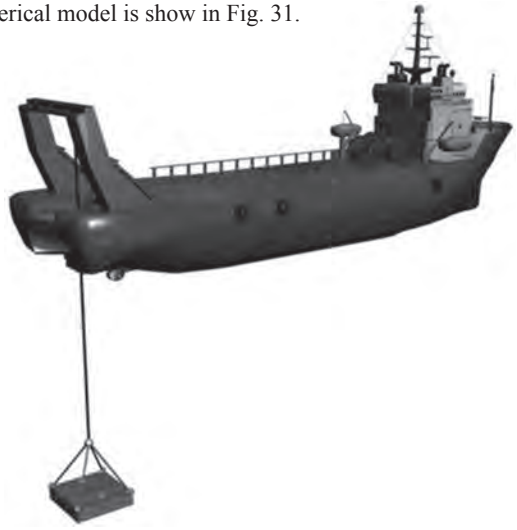

Fig. 31 TPN model for the launch of the anchor (10m lifting wire).

Regular waves - comparison with experiments

Numerical simulations with regular waves were carried out, to allow for direct comparisons with the experimental results presented in the previous section. Figure 32 shows the results when the wave period was defined as 8.83s. A very good adherence between numerical and experimental results was verified for all amplitudes considered.

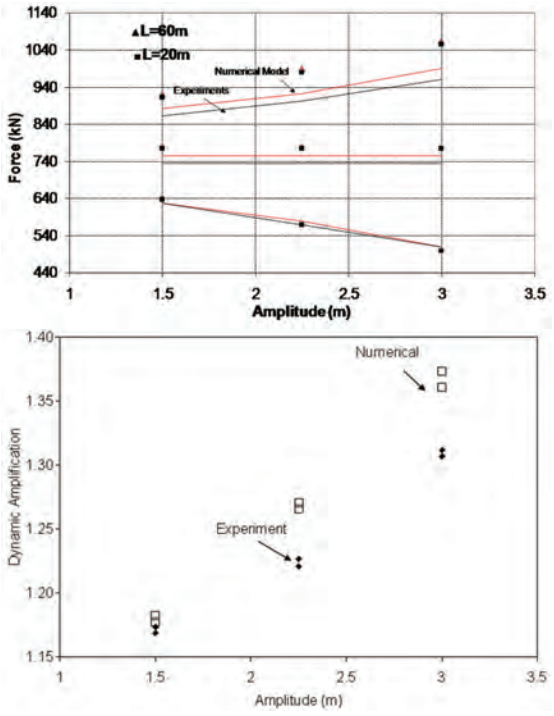

Fig. 32 Regular waves (T = 8.83s) - Case 1 - comparison between experimental and numerical simulation results.

Irregular waves - real system behavior

The behavior of the system under a real sea state was predicted by means of numerical simulations. The simulations considered several lifting wire lengths and wave significant height of 2.00m with a 9.00s peak period (Pierson-Moskowitz spectrum). Table 6 and Fig. 33 show these results. The wire traction was smaller than 1100kN for all cases without the occurrence of cable slackening. Each simulation considers 500s of operation.

Table 6 Lifting wire traction, irregular waves (Tp = 9.0s; Hs = 2.0m) – Case 1.

Lifting Wire	*Irregular Waves*			
Length (m)	F_{min} *(kN)*	F_{max} *(kN)*	F_{mean} *(kN)*	*Amp. Factor*
22.2	500	1089	774	1.4
32.2	491	1099	773	1.4
42.2	510	1079	775	1.4

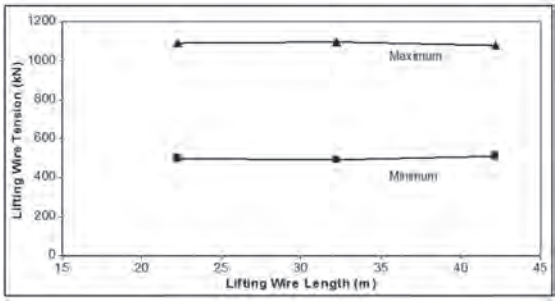

Fig. 33 Irregular waves (T p = 9.0s; Hs = 2.0m) - Case 1.

5.2 Case 2 - The launch of the anchor connected to the BTA

Several numerical simulations were carried out with the anchor directly connected to the BTA during launch in order to make comparisons with experimental results and to predict the behavior of the system under real sea conditions. The 3-D view of the numerical model is shown in Fig. 34.

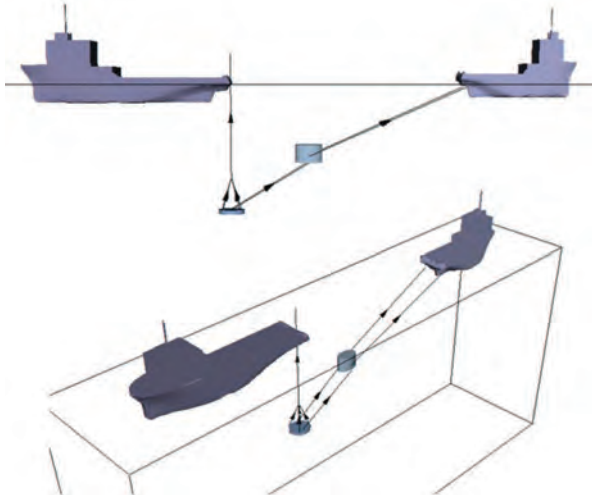

Fig. 34 TPN model for the launch of the anchor connected to the BTA - Case 2.

Regular waves - comparison with experiments

Table 7 shows the results of several numerical simulations of Case 2, considering regular waves as compared to experimental results. Such a comparison is also presented in Fig. 35. An acceptable adherence between the results was seen, except when the wave period was 5.90s, in which case the dynamic amplification factors obtained in the experiments were higher than those obtained in the numerical simulation. Such difference may be explained by the cable dynamics, since the stiffness used in the experiments was not exactly the same used in the simulations, due to practical limitations.

It is worth mentioning that for the situations with greater auxiliary tug force (196.2kN), the mean traction in the lifting wire increased (as previously shown in the static analysis), but the amplification factor decreased. The same conclusion was drawn in the experimental analysis.

The time series of the lifting wire traction for the case BEPA450830A is shown in Fig. 36. It corresponds to the case with regular wave of 2.25m amplitude and 11.78s period, lifting wire length of 60m and Faux=98kN. For this numerical simulation case, the maximum value was taken as the mean of the peak values. This value was chosen since a large variability was observed, due to numerical convergence problems in the integration of the cable numerical model. The mean (dashed line) and maximum (continuous line) values of the traction are also indicated on the plots.

It must be stressed that, although the dynamic amplification factors were very similar for the experimental and numerical results, the absolute values of the mean and maximum tractions were not very close. Such discrepancies may be explained by differences in the static configuration of the experiments. A visual (and rough) procedure was used in the initial experimental set-up, and the static configurations presented in Fig. 12 and 14 could not be reproduced accurately.

Table 7 Lifting Wire Traction - Numerical and Experimental Results - Regular waves - Case 2.

					Numerical Results - TPN				*Experimental Results*			
Test	*L (m)*	*Amp (m)*	*T (s)*	*F_{aux} (kN)*	*F_{min} (kN)*	*F_{max} (kN)*	*F_{mean} (kN)*	*Amp. Factor*	*F_{min} (kN)*	*F_{max} (kN)*	*F_{mean} (kN)*	*Amp. Factor*
BEPA45 12 30 A	60	2.25	5.90	98.1	0	1593	284	5.6	0	2342	265	8.9
BEPA45 08 30 A	60	2.25	8.80	98.1	0	1102	338	3.3	25	774	253	3.1
BEPA45 06 30 A	60	2.25	11.78	98.1	0	863	336	2.6	83	466	252	1.8
BEPA45 12 60 A	60	2.25	5.90	196.2	0	2418	461	5.2	13	1970	293	6.7
BEPA45 08 60 A	60	2.25	8.80	196.2	83	769	381	2.0	73	600	279	2.1
BEPA45 06 60 A	60	2.25	11.78	196.2	105	721	381	1.9	143	439	280	1.6
BEPD 45 12 30 A	100	2.25	5.90	98.1	0	1928	291	6.6	0	2231	242	9.2
BEPD 45 08 30 A	100	2.25	8.80	98.1	0	1046	300	3.5	21	1014	231	4.4
BEPD 45 06 30 A	100	2.25	11.78	98.1	0	720	296	2.4	69	461	231	2.0

Irregular waves - real system behavior

The behavior of the systems under real sea conditions was predicted by means of numerical simulations. The simulations considered several lifting wire lengths, and a 2.0m wave height with a 9.0s peak period (Pierson-Moskowitz spectrum). Table 8 presents the results of the simulations, which took into account the lifting wire, tether tractions and the geometrical configuration of the systems (distance and angle of BTA and lifting wire, as defined in Fig. 12). It could be seen that for all cases, there was no risk of collision between the BTA and the lifting wire. The minimum distance between BTA and lifting wire was 17.5m for all cases.

Figures 37, 38, 39 and 40 present the dynamic amplification factor and the maximum traction in the lifting wire and in the tether. Several operational problems could be identified from these results:

- Large forces in the tether that reached 1800kN with an amplification factor of up to 6.5;
- Lifting wire and tether slackening for almost all cases;
- An auxiliary tug force of 196.2kN that reduced the amplification factor in the lifting wire from 3 to 2.4, but increased the tether amplification factor (from 6.0 to 6.5).

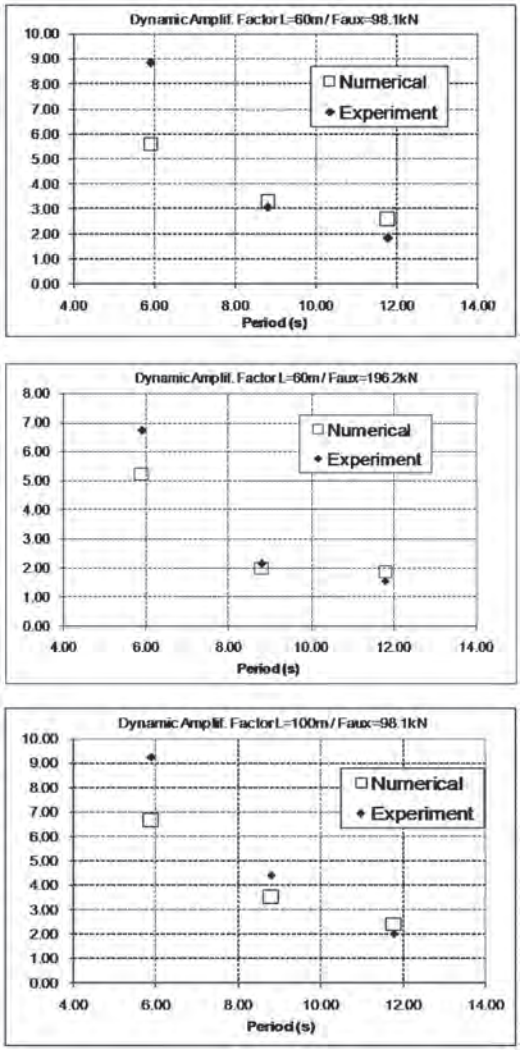

Fig. 35 Comparison of the dynamic amplification factor between experimental and numerical simulation results - Regular Waves (Case 2).

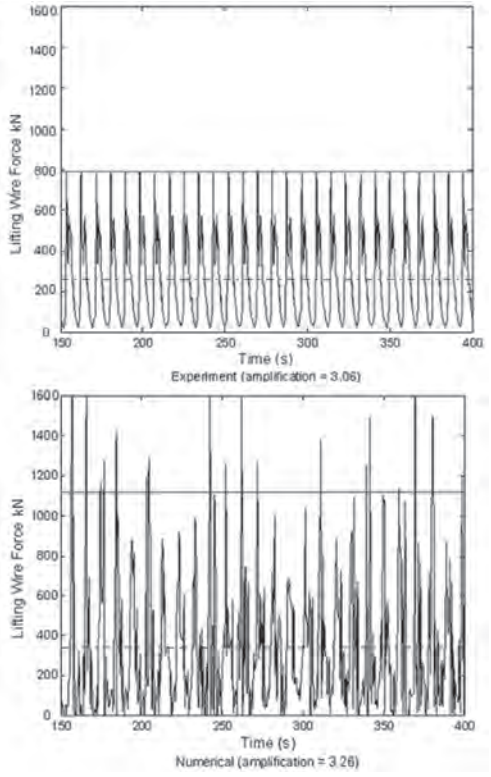

Fig. 36 Lifting wire traction - Length = 60m; Amplitude = 2.25m; Period = 8.80s; Faux = 98kN (BEPA 45 08 30A).

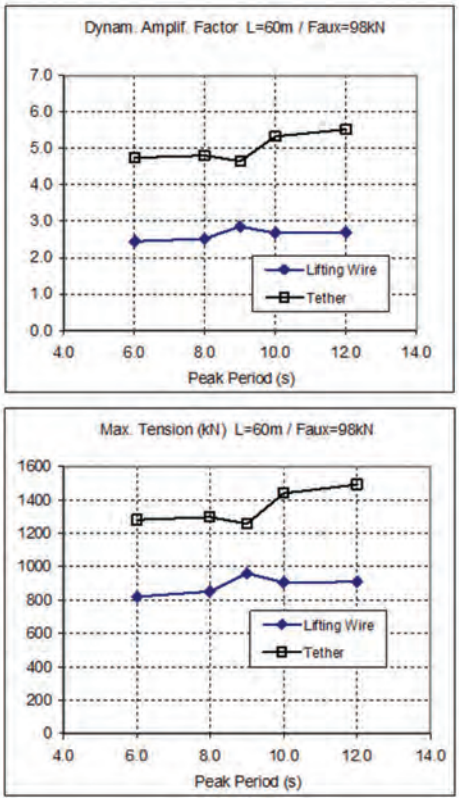

Fig. 37 Irreg. waves; Lifting wire length 60m; Faux=98kN

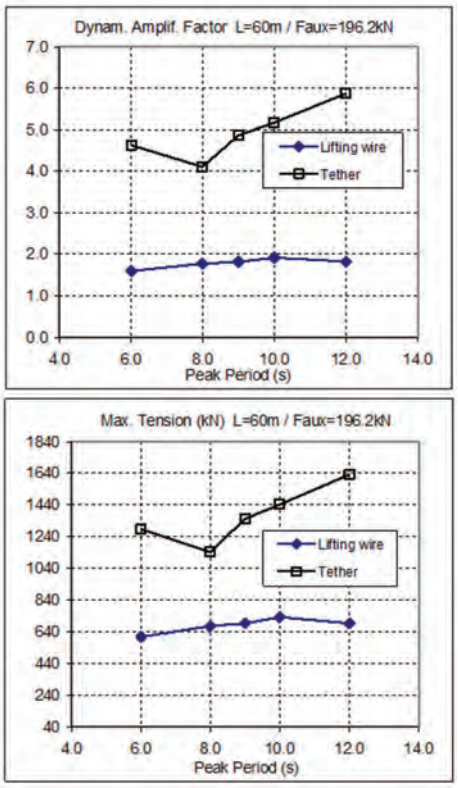

Fig. 38 Irreg. waves; Lifting wire length 60m; Faux=196.2kN

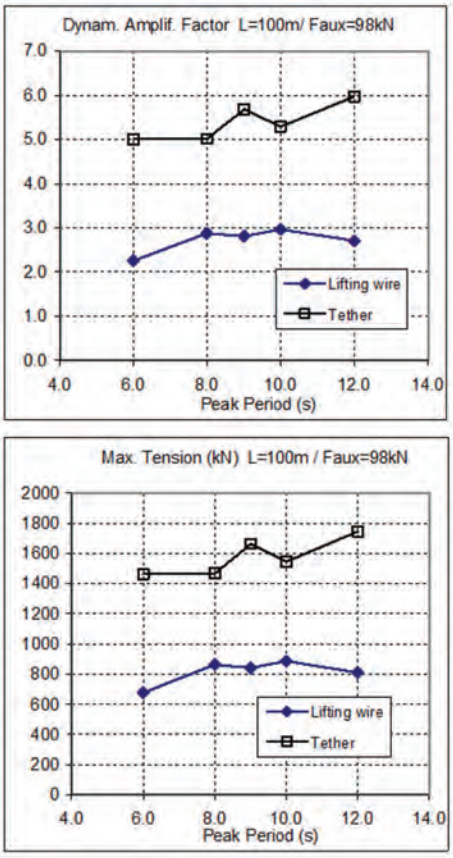

Fig. 39 - Irreg. waves; Lifting wire length 100m; Faux=98kN

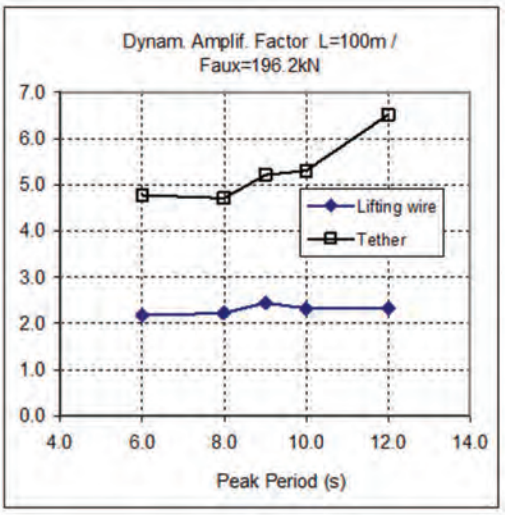

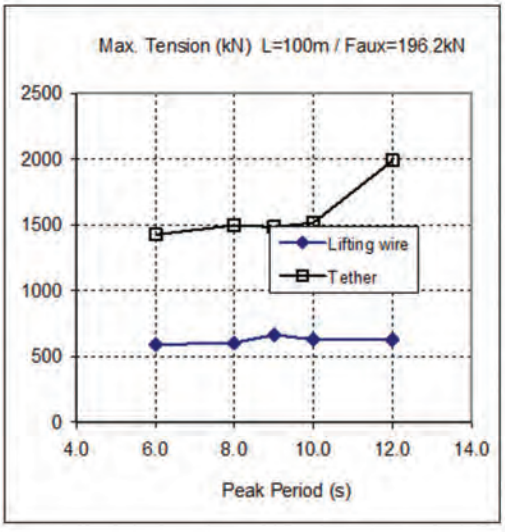

Fig. 40 Irreg. waves; Lifting wire length 100m; Faux=196.2kN

Table 8 Lifting Wire and Tether Traction - Numerical and Experimental Results - Irregular waves - Case 2.

Simulation Parameters				Lifting Wire Traction (*kN*)				Tether Traction (*kN*)				Dist.BTA-lift. wire (*m*)			Ang. BTA-lift. wire	
L(m)	*Tz(s)*	*Tp(s)*	F_{aux} *(kN)*	*Med.*	*Max.*	*Min*	*Ampl.*	*Med.*	*Max.*	*Min*	*Ampl.*	*Med.*	*Max.*	*Min*	*Med.*	*Max.*
60	4.29	6.0	98	336	820	0	2.4	270	1280	0	4.7	21	21	20	27.7	28.1
60	5.71	8.0	98	338	852	0	2.5	270	1297	0	4.8	21	22	19	28.4	29.7
60	6.43	9.0	98	336	960	0	2.9	270	1256	0	4.6	21	22	18	27.9	29.7
60	7.14	10.0	98	339	905	0	2.7	270	1439	0	5.3	21	23	18	28.2	30.5
60	8.57	12.0	98	337	909	0	2.7	270	1491	0	5.5	21	23	18	28.2	30.6
60	4.29	6.0	196.2	381	608	142	1.6	278	1287	0	4.6	36	36	34	49.4	49.8
60	5.71	8.0	196.2	382	677	122	1.8	279	1144	0	4.1	36	37	34	49.4	50.7
60	6.43	9.0	196.2	382	693	105	1.8	279	1354	0	4.9	36	37	33	49.5	51.5
60	7.14	10.0	196.2	382	734	76	1.9	279	1444	0	5.2	36	38	33	49.9	52.2
60	8.57	12.0	196.2	381	694	97	1.8	278	1634	0	5.9	36	38	33	49.7	52.3
100	4.29	6.0	98	300	677	0	2.3	292	1461	0	5.0	20	20	19	26.3	26.7
100	5.71	8.0	98	300	863	0	2.9	292	1465	0	5.0	20	20	18	26.4	27.0
100	6.43	9.0	98	299	842	0	2.8	292	1662	0	5.7	20	20	18	26.4	27.1
100	7.14	10.0	98	299	886	0	3.0	292	1545	0	5.3	20	20	18	26.4	27.3
100	8.57	12.0	98	299	810	0	2.7	292	1744	0	6.0	20	20	18	26.4	27.5
100	4.29	6.0	196.2	272	590	0	2.2	299	1426	0	4.8	35	36	34	49.1	49.6
100	5.71	8.0	196.2	272	603	0	2.2	318	1498	0	4.7	35	36	34	49.1	50.0
100	6.43	9.0	196.2	272	665	0	2.4	285	1484	0	5.2	35	36	34	49.2	50.1
100	7.14	10.0	196.2	272	632	0	2.3	285	1515	0	5.3	35	36	34	49.2	50.2
100	8.57	12.0	196.2	270	628	0	2.3	305	1987	0	6.5	35	36	34	49.2	50.3

6 New launching procedure

The experimental and numerical analysis showed that one of the launch steps (the launch of the anchor connected to the MWA) in the operation is critical for the line behavior. Since the traction in the cables may reach large values, slackening may occur. A high dynamic amplification was attained because the negative submerged weight of the MWA reduced the mean traction of the lifting wire. Therefore, the operation was considered unsafe by the engineers and by the operational staff.

The numerical simulations indicated that the slackening may occurs for 2m significative wave height. Smaller heights were not verified, so a precise weather window cannot be obtained from the analysis. However, only for an illustrative purpose, if one considers that 2m is the limiting environmental condition, such weather limitation is very restrictive considering Campos Basin scenario. In that basin, in more than 55% of the time the significant wave height is larger than 2m. During the winter, this occurrence increases to approximately 74%.

A novel procedure was proposed to prevent the launch of the MWA connected to the anchor in Case 2: launching procedure for the anchor should follow that presented in Case 1. In this case, the anchor would be launched towards the sea-floor, and a ROV would be used to adjust the fine positioning of the anchor on the sea-floor. A cable connecting the anchor to an auxiliary vessel would be used in this step to assist the anchor positioning.

Afterwards, the MWA would be launched alone using a provisory heavy chain connected to it to increase its submerged weight. The auxiliary vessel would also be used here. Thus, the MWA (and the heavy chain) would descend to the anchor, and a ROV would then connect the tethers and discard the heavy chains.

With this novel procedure, the launch of the MWA and heavy chains should demonstrate similar dynamics to that of the anchor launch in Case 1. Table 9 presents a qualitative comparison between the procedure studied in the present paper (Anchor connected to the BTA) and the new procedure (two-stages launching). In fact, the major advantage of the new procedure is related to the overall dynamics of the systems, that reduces the occurrence of cable slackening and the probability of line rupture during installation.

Table 9 Comparison between procedures for MWA installation.

	Anchor launched connected to BTA	**Two-stages launching (New Procedure)**
Time	Smaller (both anchor and BTA are launched together)	Larger time (each equipment is launched separately)
Number of vessels	2 (1 main, 1 auxiliary vessel)	2 (1 main, 1 auxiliary vessel)
ROV operation	Two operations (disconnection of lifting wire in the anchor and disconnection of assistance line in the BTA)	Several operations (disconnection of lines, heavy chain, skid installed in the BTA)
Cable slackening	Probably occurs	Small possibility of occurrence, if the heavy chain is properly dimensioned

7 Conclusions

The present paper addresses a methodology to analyze complex offshore operations involving sub-sea installation and several support vessels. Simple experiments were used to validate a numerical simulator that was then used for complex simulations of the complete installation operation under real environmental conditions.

A procedure has been proposed for the installation of a Mid Water Arch – MWA, which consists of a structure to provide riser support. The installation would involve two vessels and several cables connecting them to the MWA components.

The analysis presented showed that during one of the steps of the launch operation (the launch of the anchor connected to the MWA), the traction in the cables may reach large values, and slackening may occur.

A novel launch procedure has been proposed and successfully applied to the installation of more than 3 MWAs in the Campos Basin.

Acknowledgements

The authors gratefully acknowledge Petrobras for supporting the research project conducted at the University of São Paulo.

The second author acknowledges CNPq, the Brazilian National Research Council, Research Grant 301686/2007-6.

References

Aranha, J.A.P. (1994), "A formula for wave damping in the drift of a floating body", Journal of Fluid Mechanics, vol. 272, pp.147-155.

Faltinsen, O.M. (1990), "Sea loads on ships and offshore structures", Cambridge, Cambridge University Press, England.

Fernandes, A.C., Santos, M., Barreira, R., Ribeiro, M. (2006), "Pendulous installation method prospective model testing and numerical analysis", Proceedings of the International Conference on Offshore Mechanics and Arctic Engineering - OMAE, Hamburg, Germany.

Ferreira, M.D. (2002), "Coupled hydrodynamic analysis of an AHTS and a box structure in waves", Proceeding of International Offshore and Polar Engineering Conference, ISOPE.

Lima, J.M.T.G., Kuppens, M.L., Silveira, P.F., Stock, P.F.K. (2008), "Development of subsea facilities in the Roncador Field (P-52)", Offshore Technology Conference, OTC, Houston, TX, USA.

Santos, M., Neves, C., Sanches, C. (2009), "Y-Method for subsea equipment installation", DOT Deepwater Offshore Technology Conference, Houston, TX, USA.

Nishimoto, K., Ferreira, M., Martins, M., Masetti, I., Martins Filho, P., Russo, A., Caldo, J., and Silveira, S. (2003), "Numerical offshore tank: development of numerical offshore tank for ultra deep water oil production systems". In Proceedings of the International Conference on Offshore Mechanics and Arctic Engineering - OMAE, Cancun, Mexico.

OCIMF, (1994), "Predictions of wind and current loads on VLCCs", Oil Companies International Marine Forum.

Pinkster, J.A., (1988), "Low frequency second order wave exciting forces on floating structures", PhD Thesis, Delft University of Technology, The Netherlands.

Rowe, J.S., Mackenzie, B., Snell, R. (2001), "Deepwater installation of subsea hardware", Proceedings of the 10th Offshore Symposium, SNAME, Houston, TX, USA.

Simos, A.N. ; Tannuri, E. A. ; Pesce, C.P. ; Aranha, J. A. P.(2001), "A quasi-explicit hydrodynamic model for the dynamic analysis of a moored FPSO under current action", Journal of Ship Research, v. 45, n. 4, p. 289-301.

Tannuri, E.A., Morishita, H.M. (2006), "Experimental and numerical evaluation of a typical dynamic positioning system", Applied Ocean Research, vol. 28 pp. 133-146.

Appendix - TPN Description

The TPN is a time domain numerical procedure designed for the analysis of moored and DP offshore systems. The inputs of the simulator are:

- Floating body main parameters (dimensions, mass matrix, etc.);
- Aerodynamic drag coefficients (following standard given in OCIMF, 1994);
- Current coefficients (following standard given in OCIMF, 1994) or hydrodynamic derivatives;
- Hydrodynamic coefficients (potential damping, added mass, first and second order wave force coefficients);
- Environmental conditions (wave and wind spectra, current);
- Mooring and risers system characteristics;
- Thrusters characteristics and layout;
- DP modes and parameters.

The non-linear time-domain simulation runs in a parallel cluster computing system and outputs time series describing the motions of up to two floating unities (FU) in six degrees of freedom (6DOF), tensions on the mooring lines and hawser, propellers thrust and power, etc., and a corresponding statistical summary. 3D visualization outputs are also available.

The floating body high frequency motion (HF) due to the wave action can be evaluated in two different ways. In the simpler one the HF motion evaluated by the RAO is added to the low frequency motion (LF) that is calculated by the 3rd order Runge-Kutta integration method. Alternatively, the wave 1st order forces are applied to the body and all motion components are obtained dynamically solving the equations of motion. The current force can be evaluated through 3 different models: OCIMF Model, Cross flow Model, Maneuvering Model or Short Wing Model (Simos et al, 2001). It is possible to analyze 3D constant or oscillatory current profile. The simulator allows constant wind and gusty wind. The wind spectra implemented in the code are Harris, Wills and API. The wave can be regular and irregular. For irregular waves the spectra formulations available are Pierson-Moskowitz, JONSWAP and Gaussian. The wave first and second-order effects are modeled (see Faltinsen, 1990 and Pinkster, 1988) and wave-drift damping effects are included according to Aranha, 1994. The wave coefficients are evaluated by WAMIT (Wamit, 2000).

Three main classes of algorithms used in commercial DP systems are also implemented in TPN (Tannuri and Morishita, 2006). A low-pass filter, called wave-filter, is employed to separate high-frequency components (excited by waves) from measured signals. Such decomposition must be performed because the DP system must only control low-frequency motion, since high-frequency motion would require enormous power to be attenuated and could cause extra tear and wear in propellers. Furthermore, an optimization algorithm, called thrust allocation, must be used to distribute control forces among thrusters. It guarantees minimum power consumption to generate the required total forces and moment, positioning the vessel. At last, a control algorithm uses the filtered motion measurements to calculate such required forces and moment. Normally, a wind feedforward control is also included, enabling to estimate wind load action on the vessel (based on wind sensor measurements) and to compensate it by means of propellers. Furthermore, the simulator also includes models for propellers, taking into account their characteristics curves, being able to estimate real power consumption and delivered thrust. It also evaluates time delay between command and propeller response, caused by axis inertia.